Inorganic Chemistry

Article

Ligand-Field Photolysis of [Mo(CN)$_8$]$^{4-}$ in Aqueous Hydrazine: Trapped Mo(II) Intermediate and Catalytic Disproportionation of Hydrazine by Cyano-Ligated Mo(III,IV) Complexes

Janusz Szklarzewicz,* Dariusz Matoga, Agnieszka Kłyś, and Wiesław Łasocha

Faculty of Chemistry, Jagiellonian University, Ingardena 3, 30-060 Kraków, Poland

The substitutional photolysis of K$_4$[Mo(CN)$_8$]·2H$_2$O in 98% N$_2$H$_4$·H$_2$O has been investigated in detail. A molybdenum(II) intermediate, K$_5$[Mo(CN)$_7$]·N$_2$H$_4$, is isolated in the primary stage of the reaction that involves the oxidation of N$_2$H$_4$ to N$_2$, as evidenced by the analysis of evolving gases. The powder X-ray crystal structure of K$_5$[Mo(CN)$_7$]·N$_2$H$_4$ indicates the pentagonal bipiramidal geometry of the anion and the presence of N$_2$H$_4$ in proximity to the CN$^-$ ligands. The salt is characterized by means of EDS, IR, UV−vis, and EPR spectroscopy as well as cyclic voltammetry measurements. The secondary stages of photolysis, involving the catalytic decomposition of N$_2$H$_4$ into NH$_3$ and N$_2$, lead to the formation of a molybdenum(IV) complex, [Mo(CN)$_4$O(NH$_3$)]$^{2-}$. The monitoring of the amounts of evolving gases combined with UV−vis and EPR spectroscopic measurements at various stages of photolysis indicate that the molybdenum(III,IV) couple is catalytically active. The scheme of the catalytic decomposition of hydrazine is presented and discussed.

Introduction

The natural reduction of dinitrogen to ammonia by nitrogenases has been attracting considerable attention of chemists working on alternative systems that perform the same reaction under mild conditions.[1] Despite detailed crystallographic determination of the structure of molybdenum nitrogenase even at 1.16 Å resolution, there is still little known about the site and the mechanism of dinitrogen reduction.[1,2] Recently, trapping of intermediates formed during the reduction of nitrogenous substrates of nitrogenase (N$_2$, a diazene, hydrazine) revealed more details in this complicated process.[3] Following the strategy based on nitrogenase biomimetics, much effort has been made by researchers on models with relatively simple mononuclear

transition-metal complexes. Among them, monometallic molybdenum complexes have quite well-estabilished mechanisms of N$_2$ reduction to ammonia.[4] One wide group of these systems is based on a molybdenum in its low oxidation state [molybdenum(0)], different from biological FeMo−nitrogenase [where molybdenum(III,IV) is present], whereas the other distinctive group includes molybdenum in higher oxidation states [molybdenum(III)−molybdenum(VI)]. However, the first synthetic complex that could catalytically reduce dinitrogen under mild conditions and thus mimic nitrogenase was published only recently. Yandulov and Schrock reported a molybdenum(III) triamidoamine complex as a catalyst for the reduction of dinitrogen to ammonia at room temperature and a pressure of one atmosphere.[4c,5] In relation to these and biological N$_2$-fixing models, the late stage of dinitrogen fixation, reductive cleavage of the N−N

---

* To whom correspondence should be addressed. E-mail: szklarze@chemia.uj.edu.pl.

(1) (a) For recent reviews on dinitrogen fixation, see: Holland, P. L. In *Comprehensive Coordination Chemistry II*; McCleverty, J. A., Meyer T. J., Eds.; Elsevier: Oxford U.K., 2004; Vol. 8, Chapter 8.22, p 569. (b) MacKay, B. A.; Fryzuk, M. D. *Chem. Rev.* **2004**, *104*, 385–401. (c) Barney, B. M.; Lee, H.-I.; Dos Santos, P.; Hoffman, B. M.; Dean, D. R.; Seefeldt, L. C. *Dalton Trans.* **2006**, 2277–2284. (d) Himmel, H.-J.; Reiher, M. *Angew. Chem., Int. Ed.* **2006**, *45*, 6264–6288.

(2) (a) Einsle, O.; Tezcan, F. A.; Andrade, S. L. A.; Schmid, B.; Yoshida, M.; Howard, J. B.; Rees, D. C. *Science* **2002**, *297*, 1696–1700. (b) Howard, J. B.; Rees, D. C. *Proc. Natl. Acad. Sci. U.S.A.* **2006**, *103*, 17088–17093.

(3) (a) Barney, B. M.; Laryukhin, M.; Igarashi, R. Y.; Lee, H.-I.; Dos Santos, P.; Yang, T.-C.; Hoffman, B. M.; Dean, D. R.; Seefeldt, L. C. *Biochemistry* **2005**, *44*, 8030–8037. (b) Barney, B. M.; Yang, T.-C.; Igarashi, R. Y.; Dos Santos, P.; Laryukhin, M.; Lee, H.-I.; Hoffman, B. M.; Dean, D. R.; Seefeldt, L. C. *J. Am. Chem. Soc.* **2005**, *127*, 14960–14961.

(4) (a) For reviews, see Barriere, F. *Coord. Chem. Rev.* **2003**, *236*, 71–89. (b) Hidai, M.; Mizobe, Y. *Met. Ions Biol. Syst.* **2002**, *39*, 121–161. (c) Schrock, R. R. *Acc. Chem. Res.* **2005**, *38*, 955–962. (d) Tuczek, F. *Adv. Inorg. Chem.* **2004**, *56*, 27–53.

bond in hydrazine leading to ammonia has also been studied, but the reported complexes (both mono and multimetallic) that catalyze this process are still very limited.[6,7]

In the 1970s, it was shown that tetracyanooxo complexes of molybdenum(IV) can be precursors for a reduction of dinitrogen to hydrazine and ammonia, but the efficiency of these systems under studied conditions was relatively low.[8] On the other hand, working with molybdenum complexes we have observed that several molybdenum(IV) tetracyanooxo complexes are involved in redox processes in the presence of O$_2$ and NO molecules.[9,10] In the reactions with molecular oxygen, the molybdenum(IV) center is oxidized to molybdenum(VI), and attempts have been made to utilize this process in the oxidation of other molecules.[11] These attempts to build an efficient catalytic system based on a cyanooxo molybdenum(IV/VI) redox couple proved to be unsuccessful so far, and the difficulty of quantitative reduction of molybdenum(VI) species to molybdenum(IV) was suggested as a main hindrance.[11c] Recently, we decided to further explore the redox chemistry of molybdenum(IV) cyano complexes, this time under reducing conditions. In our previous article, it has been shown that a prolonged $d-d$ photolysis of [Mo(CN)$_8$]$^{4-}$ in N$_2$H$_4$·H$_2$O leads to an almost quantitative formation of molybdenum(IV) complex [Mo(CN)$_4$-

O(NH$_3$)]$^{2-}$ as a final product. The photolysis is accompanied by catalytic, quantitative disproportionation of hydrazine into NH$_3$ and N$_2$.[12] However, it was not clear which complexes (substrates, intermediates, or products) are catalytically active. For comparison, in the photolysis of aqueous [Mo(CN)$_8$]$^{4-}$ solution, stepwise cyano ligand release is observed with the formation of hepta-, hexa-, and pentacyano intermediates; and in all described complexes, the oxidation state of molybdenum remains intact.[13]

In this work, we report the detailed study on the ligand-field photolysis of [Mo(CN)$_8$]$^{4-}$ in aqueous hydrazine that provides a deeper insight in the catalytic mechanism of N$_2$H$_4$ decomposition. The same oxidation state (IV) of the metal center in the substrate and final products of the photolysis was intriguing, given that hydrazine transformations are redox processess, and prompted us to investigate the role of metal in the catalytic decomposition of the solvent. In particular, our goal was to find isolable intermediates as well as to determine which transient species in a route from octa- to tetra-cyano complexes are catalytically active in the studied system. These findings were expected to be important steps in attempts to utilize molybdenum(IV) cyanocomplexes toward efficient dinitrogen reduction.

Experimental Section

K$_4$[Mo(CN)$_8$]·2H$_2$O,[12](PPh$_4$)$_2$[Mo(CN)$_4$O(NH$_3$)]·2H$_2$O,[12]Cs$_2$Na-[Mo(CN)$_5$O],[14] K$_3$Na[Mo(CN)$_4$O$_2$]·6H$_2$O,[15] and K$_5$[Mo(CN)$_7$]·H$_2$O[16] were prepared according to literature procedures, their identities and purity confirmed by elemental analyses and IR spectroscopy. All other chemicals including hydrazine monohydrate (98%, Aldrich) were of analytical grade and were used as supplied.

Carbon, hydrogen, and nitrogen were determined using Euro EA 3000 elemental analyzer. The UV−vis absorption spectra were recorded on a Shimadzu UV-2101PC scanning spectrophotometer in the 200−900 nm range. Diffuse reflectance spectra were measured in BaSO$_4$ pellets with BaSO$_4$ as a reference using a Shimadzu 2101 PC spectrometer equipped with an ISR-260 attachment. The IR spectra were recorded as either KBr pellets or nujol mulls on a Bruker EQUINOX 55 FTIR spectrometer. The thermogravimetric analyses were performed on a TGA/SDTA (Mettler Toledo) microthermogravimeter with a quadrupole mass spectrometer Thermostar GSD 300T (Balzers). X-band ESR spectra were recorded at liquid nitrogen and at room temperature on a Bruker ELEXSYS E-500CW-EPR spectrometer operating at 9.1 GHz and a modulation frequency of 100 kHz. Cyclic voltammetry measurements were carried out under argon in aqueous solutions with KNO$_3$ (0.10 M) or KCN (0.10 M) as the supporting electrolytes using a platinum working and counting and Ag/AgCl reference electrodes on a model EA9 electrochemical analyzer. The redox potentials were calibrated versus K$_4$[Fe(CN)$_6$], which was used as

(5) (a) Yandulov, D. V.; Schrock, R. R. *Science* **2003**, *301*, 76–78. (b) Yandulov, D. V.; Schrock, R. R.; Rheingold, A. L.; Ceccarelli, C.; Davis, W. *Inorg. Chem.* **2003**, *42*, 796–813. (c) Ritleng, V.; Yandulov, D. V.; Weare, W. W.; Schrock, R. R.; Hock, A. S.; Davis, W. M. *J. Am. Chem. Soc.* **2004**, *126*, 6150–6163. (d) Yandulov, D. V.; Schrock, R. R. *Inorg. Chem.* **2005**, *44*, 1103–1117. (e) McNaughton, R. L.; Chin, J. M.; Weare, W. W.; Schrock, R. R.; Hoffman, B. M. *J. Am. Chem. Soc.* **2007**, *129*, 3480–3481. (f) Magistrato, A.; Robertazzi, A.; Carloni, P. *J. Chem. Theory Comput.* **2007**, *3*, 1708–1720.
(6) (a) For reactions on monometallic sites, see: Chu, W.-C.; Wu, C.-C.; Hsu, H.-F. *Inorg. Chem.* **2006**, *45*, 3164–3166. (b) Hitchcock, P. B.; Hughes, D. L.; Maguire, M. J.; Marjani, K.; Richards, R. L. *J. Chem. Soc., Dalton Trans.* **1997**, 4747–4752. (c) Block, E.; Ofori-Okai, G.; Kang, H.; Zubieta, J. *J. Am. Chem. Soc.* **1992**, *114*, 758–759. (d) Schrock, R. R.; Glassman, T. E.; Vale, M. G.; Kol, M. *J. Am. Chem. Soc.* **1993**, *115*, 1760–1772. (e) Schrock, R. R.; Glassman, T. E.; Vale, M. G. *J. Am. Chem. Soc.* **1991**, *113*, 725–726. (f) Vale, M. G.; Schrock, R. R. *Inorg. Chem.* **1993**, *32*, 2767–2772.
(7) (a) For reactions on multimetallic sites, see: Demadis, K. D.; Malinak, S. M.; Coucouvanis, D. *Inorg. Chem.* **1996**, *35*, 4038–4046. (b) Coucouvanis, D.; Demadis, K. D.; Malinak, S. M.; Mosier, P. E.; Tyson, M. A.; Laughlin, L. J. *J. Mol. Catal.* **1996**, *107*, 123–135. (c) Malinak, S. M.; Demadis, K. D.; Coucouvanis, D. *J. Am. Chem. Soc.* **1995**, *117*, 3126–3133. (d) Demadis, K. D.; Coucouvanis, D. *Inorg. Chem.* **1995**, *34*, 3658–3666. (e) Demadis, K. D.; Coucouvanis, D. *Inorg. Chem.* **1994**, *33*, 4195–4197. (f) Coucouvanis, D.; Mosier, P. E.; Demadis, K. D.; Patton, S.; Malinak, S. M.; Kim, C. G.; Tyson, M. A. *J. Am. Chem. Soc.* **1993**, *115*, 12193–12194.
(8) (a) Robinson, P. R.; Moorehead, E. L.; Weathers, B. J.; Ufkes, E. A.; Vickrey, T. M.; Schrauzer, G. N. *J. Am. Chem. Soc.* **1976**, *98*, 2815–2822. (b) Schrauzer, G. N.; Robinson, P. R.; Moorehead, E. L.; Vickrey, T. M. *J. Am. Chem. Soc.* **1975**, *97*, 7069–7076. (c) Moorehead, E. L.; Robinson, P. R.; Vickrey, T. M.; Schrauzer, G. N. *J. Am. Chem. Soc.* **1976**, *98*, 6556–6601. (d) Robinson, P. R.; Moorehead, E. L.; Weathers, B. J.; Ufkes, E. A.; Vickrey, T. M.; Schrauzer, G. N. *J. Am. Chem. Soc.* **1977**, *99*, 3657–3662.
(9) (a) Matoga, D.; Szklarzewicz, J.; Samotus, A.; Lewiński, K. *J. Chem. Soc., Dalton Trans.* **2002**, 3587–3592. (b) Matoga, D.; Szklarzewicz, J.; Samotus, A.; Burgess, J.; Fawcett, J.; Russell, D. R. *Polyhedron* **2000**, *19*, 1503–1509.
(10) Matoga, D.; Szklarzewicz, J.; Fawcett, J. *Polyhedron* **2005**, *24*, 1533–1539.
(11) (a) Arzoumanian, H.; Petrignani, Jean, F.; Pierrot, M.; Ridouane, F.; Sanchez, J. *Inorg. Chem.* **1988**, *27*, 3377–3381. (b) Arzoumanian, H. *Coord. Chem. Rev.* **1998**, *178*, 191–202. (c) Matoga, D. Ph.D. Thesis, Jagiellonian University, Kraków, Poland, 2003.

(12) Szklarzewicz, J.; Matoga, D.; Lewiński, K. *Inorg. Chim. Acta* **2007**, *360*, 2002–2008.
(13) (a) Szklarzewicz, J.; Matoga, D.; Niezgoda, A.; Yoshioka, D.; Mikuriya, M. *Inorg. Chem.* **2007**, *46*, 9531–9533. (b) Matoga, D.; Szklarzewicz, J.; Samotus, A.; Burgess, J.; Fawcett, J.; Russell, D. R. *Transition Met. Chem.* **2001**, *26*, 404–411. (c) Samotus, A.; Szklarzewicz, J. *Coord. Chem. Rev.* **1993**, *125*, 63–74.
(14) Dudek, M.; Samotus, A. *Transition Met. Chem.* **1985**, *10*, 271–274.
(15) Samotus, A.; Dudek, M.; Kanas, A. *J. Inorg. Nucl. Chem.* **1975**, *37*, 943–948.
(16) Drew, M. G. B.; Mitchell, P. C. H.; Pygall, C. F. *J. Chem. Soc., Dalton Trans.* **1977**, 1071–1077.

an internal potential standard to avoid the influence of liquid junction potential. $E^0_{1/2}$ values were calculated from the average anodic and cathodic peak potentials, $E^0_{1/2} = 0.5(E_a + E_c)$; the final values of potentials were reported versus standard hydrogen electrode (SHE). The scanning electron microscope JSM 5410 JEOL (at 20 keV) was used to verify purity of samples as well as to estimate the K/Mo ratio using an EDS 679A-3SES energy dispersive X-ray spectrometer (Noran Instruments Inc.); $K_4[Mo(CN)_8] \cdot 2H_2O$ and KI were used as standards.

Continuous photolyses for synthetic purposes were performed using a low-pressure mercury lamp. Spectral changes were recorded for solutions irradiated with a low-pressure mercury lamp in glass conical flasks to prevent them from UV irradiation. The amount of N_2 released during photolysis was measured in a gas burette using 1.0 M HCl as an NH_3 trap. The yield of conversion of N_2H_4 into NH_3 was established on the basis of the amount of evolved N_2 and NH_3. To estimate the amount of released NH_3 the reacting mixtures, each was photolyzed for a certain period of time, and was alkalized with 6.0 M NaOH and heated until boiling. The evolving gas (NH_3) was passing through an NH_3 trap filled with 25.00 mL of 0.1000 M HCl. Such solutions were subsequently transferred quantitatively to Erlenmeyer flasks and subjected to potentiometric titrations carried out with 0.0971 M NaOH on a Schott Titroline Alpha titrator.

The rates of N_2 evolution were measured in 1.00 cm quartz cuvettes. $K_4[Mo(CN)_8] \cdot 2H_2O$ (0.200 g) was dissolved in $N_2H_4 \cdot H_2O$ (98%, 1.5 mL) and irradiated as described above for a certain period of time. The irradiation was stopped, and a cuvette was connected to a gas burette. After that, the cuvette with solution was heated to 90 ± 1 °C, thermostatted for 5 min, and then the rate of N_2 evolution was measured. The procedure was repeated for various irradiation times.

A catalytic activity of $K_4[Mo(CN)_8] \cdot 2H_2O$ and that of its photoproducts (including $K_5[Mo(CN)_7] \cdot N_2H_4$, $Cs_2Na[Mo(CN)_5]$, $(PPh_4)_2[Mo(CN)_4O(NH_3)] \cdot 2H_2O$, and $K_3Na[Mo(CN)_4O_2] \cdot 6H_2O$) was investigated under the same conditions as described for irradiated $K_4[Mo(CN)_8] \cdot 2H_2O$ solutions (with the same concentration of molybdenum complexes), except that the solutions were not exposed to irradiation prior to thermostatting.

Synthesis of $K_5[Mo(CN)_7] \cdot N_2H_4$ (1). $K_4[Mo(CN)_8] \cdot 2H_2O$ (1.01 g, 2.03 mmol) and KI (2.00 g, 12.1 mmol) were dissolved in $N_2H_4 \cdot H_2O$ (98%, 7.5 mL, 0.15 mol). The solution in an Erlenmeyer flask was exposed to sunlight for a period of one day or was irradiated with the low-pressure mercury lamp for 30 min. The resulting product of **1** (yield: 0.71 g, 69%) was filtered off, washed with EtOH and Me_2CO, and dried. All manipulations were performed under argon.

Synthesis of $K_5[Mo(CN)_7] \cdot H_2O$ (2). The salt was prepared according to two different methods, one described in the literature[16] and the other presented below. $K_5[Mo(CN)_7] \cdot N_2H_4$ (0.50 g, 0.99 mmol) was dissolved in 50% $N_2H_4(aq)$ (5.0 mL) and precipitated with acetone. The crystalline product of **2** (yield: 0.40 g 82%) was filtered off, washed with acetone, diethyl ether and dried. All of the manipulations were performed under argon. Anal. Calcd for $C_7H_2K_5MoN_7O$: C, 17.1; H, 0.4; N, 20.0. Found: C, 17.5; H, 0.5; N, 19.7%. The purity of the compound was verified using IR and UV−vis spectroscopy.

Caution! *During handling and photolysis of the cyano complexes, care should be taken because of HCN release. N_2H_4 is carcinogenic and contact with it should be limited.*

Crystal structure determination of 1. The polycrystalline samples of **1** were measured on a Bruker D5005 and a Philips X'pert diffractometer under mineral oil. The angle measuring range was

5−85° (2θ) with 0.02° resolution, measuring time 14 s/step, applied lamp voltage 40 kV, with 30 mA cathodic current. The space group and cell parameters were determined with *PROSZKI* package with *TREOR* and *VISSER* software.[17] The lattice parameters were refined with *APPLE* software using type I net extinctions $h + k + l = 2n + 1$ according to the found space group.[18] Because of the similarities between structures of **1** and $K_4[Mo(CN)_7] \cdot H_2O$, database data for the latter compound were used as a starting model in *FOX* software and in calculations within the Rietveld method.[16,19]

Results and Discussion

General Description of the Photolysis. It has been previously observed that the irradiation of $K_4[Mo(CN)_8] \cdot 2H_2O$ solution in 98% $N_2H_4 \cdot H_2O$ yields the color change from yellow to orange-yellow, green, and finally blue.[12] From the final blue solution, the $[Mo(CN)_4O(NH_3)]^{2-}$ complex can be isolated nearly quantitatively. It has also been found that during the $[Mo(CN)_8]^{4-}$ photolysis, N_2H_4 decomposes with N_2 and NH_3 formation.[12] In this work, we have found that the proper modification of conditions leads to the precipitation of an orange-yellow product (**1**) at the very early stage of the photolysis. The formation of the solid primary photoproduct $K_5[Mo(CN)_7] \cdot N_2H_4$ has been observed both in the presence of electrolytes such as KCl, KI, K_2CO_3 or K_2SO_4 as well as when the concentration of starting $K_4[Mo(CN)_8] \cdot 2H_2O$ in 98% $N_2H_4 \cdot H_2O$ has been relatively high ($c > 0.3$ M). The photolytic formation of **1** is represented by eqs 1−3.

$$[Mo(CN)_8]^{4-} \xrightarrow{h\nu} {}^*[Mo(CN)_8]^{4-} \tag{1}$$

$$^*[Mo(CN)_8]^{4-} \rightarrow [Mo(CN)_7]^{3-} + CN^- \tag{2}$$

$$[Mo(CN)_7]^{3-} + 1/2\ N_2H_4 \rightarrow [Mo(CN)_7]^{5-} + 1/2\ N_2 + 2H^+ \tag{3}$$
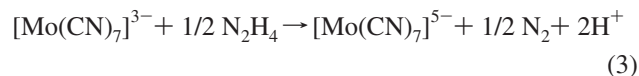
The introduction of salts with other countercations than K^+ (e.g., NaCl, CsCl, LiCl) to the photolyzed system also results in the precipitation of a yellow-orange product at the early stage of photolysis but the most suitable crystals for X-ray diffraction experiment have been obtained in the presence of KI. The oxidation of N_2H_4 to N_2 has been demonstrated by the volumetric measurements of the evolved N_2 combined with the determination of the amount of produced NH_3. It has been found that at the early stage of photolysis (when **1** is formed) almost pure N_2 is evolved. The traces of NH_3 are formed due to the catalytic activity of **1**, which is discussed later in this article.

Characterization of the Primary Photoproduct. Isolated, diamagnetic **1** is a crystalline yellow-orange solid that is soluble in water, merely soluble in hydrazine hydrate, and

(17) (a) Łasocha, W.; Lewiński, K. *J. Appl. Crystallogr.* **1994**, *27*, 437–438. (b) Werner, P. E.; Eriksson, L.; Westdahl, M. *J. Appl. Crystallogr.* **1985**, *18*, 367–370. (c) Visser, J. W. *J. Appl. Crystallogr.* **1969**, *2*, 89–95.

(18) Appleman D. E., Jr. Indexing and least squares refinement of powder diffraction data. U.S. National Technical Information Service, Document PB 216−188, 1973, Job 9214.

(19) Favre-Nicolin, V.; Cerny, R. *J. Appl. Crystallogr.* **2002**, *35*, 734–743.
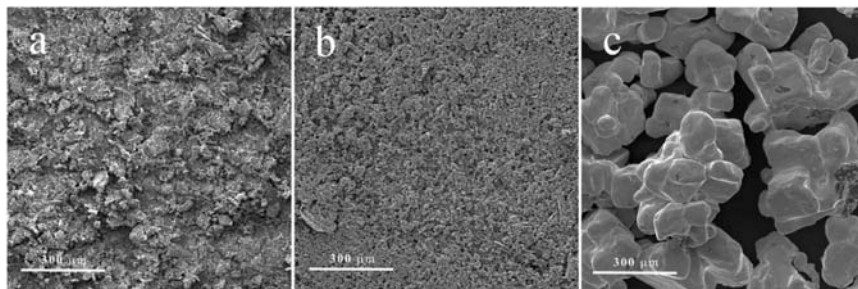
Figure 1. Scanning electron microscope photographs of (a) KI, (b) $K_5[Mo(CN)_7] \cdot N_2H_4$, and (c) $K_4[Mo(CN)_8] \cdot 2H_2O$.
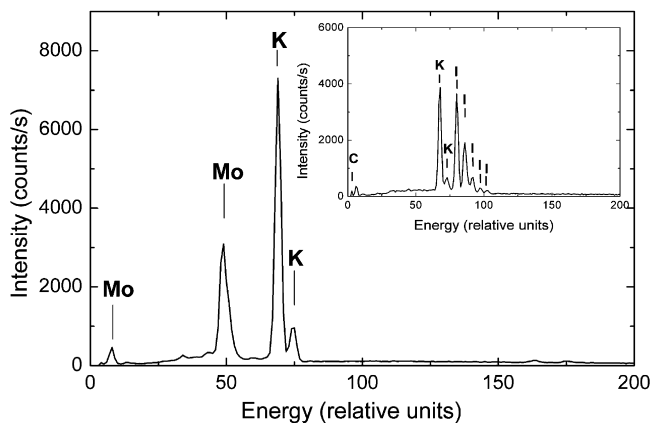
Figure 2. EDS spectrum of $K_5[Mo(CN)_7] \cdot N_2H_4$ (**1**). In the upper right corner, the EDS spectrum of KI is presented for comparison.
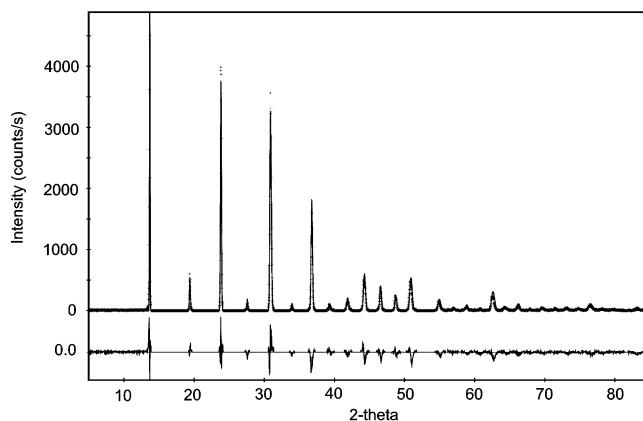
Figure 3. Diffractogram of $K_5[Mo(CN)_7] \cdot N_2H_4$ (**1**) and differential curve obtained by Rietveld calculations.

Figure 4. Structure of the $[Mo(CN)_7]^{5-}$ ion in **1**.

insoluble in organic solvents. It is unstable in air and it becomes green. At room temperature, the salt is stable when kept under $N_2H_4 \cdot H_2O$, and the dry compound undergoes slow decomposition with NH_3 release even under argon. This process has considerably affected the results of elemental analyses, making them not repeatable. Each measurement performed on samples of **1** has shown that carbon and nitrogen contents are between those calculated for **1** and **2**. These results indicate weak bonding of the N_2H_4 molecule and its release during handling. Repeated crystallizations of **1** from water or diluted N_2H_4 solutions always lead to the quantitative formation of $K_5[Mo(CN)_7] \cdot H_2O$, which confirms the weak bonding of N_2H_4 group and indicates that N_2H_4 is released upon dissolving, thus it acts as an outer-sphere solvent molecule in the adduct **1**. In aqueous solutions, **1** undergoes dissociation and the $[Mo(CN)_7]^{2-}$ anion is stable under anaerobic conditions (no spectral changes observed), whereas in the presence of dioxygen the solution changes color from yellow to red. In spite of many efforts, we were not able to get single crystals of **1** suitable for X-ray measurements, thus the structure was refined using powder diffractograms. To verify the purity of the sample, and in particular to exclude the presence of KI cocrystallizing with salt **1,** we used the scanning electron microscope equipped with an energy dispersive X-ray spectrometer. The salts KI and $K_4[Mo(CN)_8] \cdot 2H_2O$ were used as references. The SEM photograph of **1** presented in Figure 1 indicates that the sample is uniform. The EDS spectra show that **1** does not contain KI (Figure 2) and that the salt composition is the same in crystals and within studied surfaces.
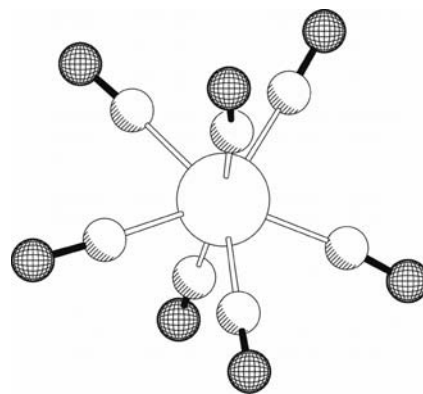
The established K/Mo ratio for **1** was found to be 5.6, and this value was estimated on the basis of the K/Mo ratio (4.0) for the $K_4[Mo(CN)_8] \cdot 2H_2O$ standard. The difference between the observed and expected value (5.0) for **1** is the result of complicated surface morphology. The surface of the sample is not flat, and thus the results of quantitative EDS measurements can only be interpreted tentatively.

Structure of $K_5[Mo(CN)_7] \cdot N_2H_4$. The powder diffractogram of **1** is presented in Figure 3, and the structure of the complex anion in **1** is presented in Figure 4. Because of the pseudoregular symmetry of the unit cell, the unusual instability of the Rietveld method as well as the softness of the molecule and easy deformation of the M−CN angles are observed (angles even as low as 140° are observed if very soft restraints are introduced in calculations). The attempts to solve the structure using higher symmetry (for example *Imm*2 or *I*222) were unsuccessful. On the other hand,
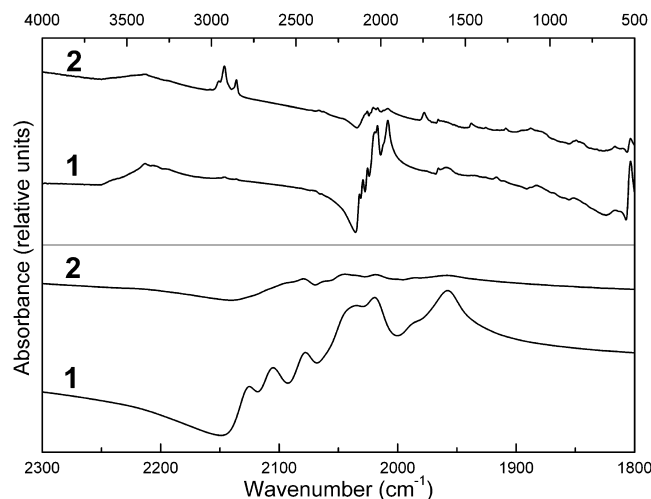
Figure 5. IR spectra of $K_5[Mo(CN)_7] \cdot N_2H_4$ (**1**) and $K_5[Mo(CN)_7] \cdot H_2O$ (**2**) (in KBr).

Figure 6. (a) Electronic spectra of $K_5[Mo(CN)_7] \cdot N_2H_4$ (**1**): in aqueous solution (dotted line, $c = 1.5 \times 10^{-3}$ M, $d = 1.00$ cm) and diffuse reflectance (solid line, after Kubelka−Munk transformation). (b) UV−vis spectra of $K_5[Mo(CN)_7] \cdot N_2H_4$ (**1**) in H_2O ($c = 5.0 \times 10^{-3}$ M, $d = 0.500$ cm): initial spectrum (dotted line); after short exposure to dioxygen (dashed line), final spectrum (solid line). (c) Spectral changes of oxidized aqueous solution of **1** induced by the addition of KCN. The arrows indicate direction of the changes ($c = 5.0 \times 10^{-3}$ M, $d = 0.500$ cm, spectra recorded every 180 s).

similarity of the composition and unit cell dimensions of **1** suggest its close relation to the structure of the compound described by Drew et al.[16] The literature cell volume for the latter was 754.08, whereas for **1** it was found as 768.1(2) Å³. This similarity was confirmed by the Rietveld method using for computation the parameters of the net, line shape, scale factor, and zero 2θ scale parameters. The resulting factors are: $R_F = 11.5$, R_{wp} (weight profile) = 14.2%. On the basis of the partially refined model, the differential Fourier maps were calculated and localization of atoms was obtained, for N11 they are 0.000, 0.261, and 0.0. The site occupancy of N11 is equal to 50%. The Fourier maps indicate the possibility of other atom locations, for instance in $(0,x,0)$ or $(0,0,z)$ positions.

The cell parameters were found as $a = 9.167(1)$, $b = 9.187(13)$, and $c = 9.121(3)$ Å; $\alpha = \beta = \gamma = 90°$. The calculated unit cell volume 768.1(2) Å³ indicates the presence of a molecule bigger than H_2O and giving a more complicated hydrogen-bond network. The ion symmetry is a distorted pentagonal bipyramid, close to the structure of the anion found by Drew et al.[16] The cyano ligands are almost linear, with not more than 10° deviations of the Mo−CN bonds from linearity.

The isolated salt **1** is formed only in concentrated $N_2H_4 \cdot H_2O$. It was found earlier that the photolysis of $K_4[Mo(CN)_8] \cdot 2H_2O$ in diluted aqueous N_2H_4 solutions is very similar to the one without hydrazine, and a salt of formula $Cd_2[Mo(CN)_8] \cdot 2N_2H_4 \cdot 4H_2O$ was isolated and structurally characterized from such solutions.[20]

IR Spectra. The IR spectrum of **1** is presented in Figure 5, and the spectrum of $K_5[Mo(CN)_7] \cdot H_2O$ is given for comparison. The band at 523 cm⁻¹ can be assigned to the ν_{Mo-C} absorption, and the other bands below 650 cm⁻¹ can be attributed to δ_{MoCN} vibrations. The characteristic bands of N_2H_4 are observed in the 650−900 cm⁻¹ range (out-of-plane ν_{N-H}), at 1081 cm⁻¹ (ν_{N-N} stretching), at 1610 and 1660 cm⁻¹ (δ_{NH2}), and in the 3000−3650 cm⁻¹ range (ν_{N-H}).

The observed small shift of these bands in comparison to that of $N_2H_4 \cdot H_2O$ is the result of the interaction of N_2H_4 with cyano ligands, probably via a network of hydrogen bonds.

In the ν_{CN} range, there are seven bands at 1958, 1985, 2019, 2034, 2078, 2107, and 2125 cm⁻¹. In the literature, there are different IR data on **2**, probably due to problems with purification and proper handling with that very unstable salt.[16,21] Our investigations indicate that samples of salt **2** prepared by us in two different methods have the same IR and UV−vis spectra, and these were taken for comparison with the respective spectra of **1**. It can be seen that in the ν_{CN} range there is a significant difference between **1** and **2** (Figure 5). Salt **1** has seven bands with two new bands above 2100 cm⁻¹, not observed in **2**. The presence of seven bands in this region indicates low symmetry of the anion in **1** (C_1), very similar to that observed in $K_5[Mo(CN)_7] \cdot H_2O$. On the other hand, band positions are closer to those found for $Na_5[Mo(CN)_7] \cdot 10H_2O$ (ranging from 1968 to 2142 cm⁻¹).[16,21]

UV−vis Spectra. The aqueous solution electronic spectrum of **1**, presented in Figure 6, is almost identical with the spectrum of a solution of $K_4[Mo(CN)_8] \cdot 2H_2O$ in $N_2H_4 \cdot H_2O$, irradiated for 10 min. It has a shoulder at 420 nm, and at higher energies a continuous increase of absorbance, not featuring any bands, is observed, similarly as it is for **2**. The shoulder at 420 nm is attributable to a d−d transition due to

(20) Chojnacki, J.; Grochowski, J.; Lebioda, Ł.; Oleksyn, B.; Stadnicka, K. *Rocz. Chem., Ann. Soc. Chim. Polonorum* **1969**, *43*, 273−280.

(21) Soares, A. M.; Griffith, W. P. *J. Chem. Soc., Dalton Trans.* **1981**, 1886−1891.

its low intensity. In diluted deoxygenated aqueous solutions, spectra of **1** and **2** are identical, which indicates weak interactions of N_4H_4 with the $[Mo(CN)_7]^{5-}$ ion and its release upon dissolving.

The diffuse reflectance spectrum of **1**, shown in part a of Figure 6, reveals bands at 325, 365, and 430 nm, and in this region the spectrum is similar to that of $K_5[Mo(CN)_7]\cdot H_2O$.[16] The increase of absorbance above 700 nm, neither observed in the reflectance spectrum of **2** nor in that of aqueous solution of **1**, is associated with the interaction of the N_2H_4 molecule with cyano ligands and suggests its SMCT (solvent-to-metal charge transfer) origin.

Reaction of $K_5[Mo(CN)_7]\cdot N_2H_4$ with O_2. The complex ion in **1** is stable in deoxygenated aqueous solution. In the presence of dioxygen, the originally yellow solution turns red. The electronic spectra of an aqueous solution of **1** reacting with O_2 are presented in part b of Figure 6. When the reaction is completed, the spectrum shows bands of relatively low intensities at 500 and 600 nm. The latter can be attributed to the formation of tetracyanooxocomplexes of molybdenum(IV), whereas the band at 500 nm, observed also in irradiated solutions of $K_4[Mo(CN)_8]\cdot 2H_2O$, is associated with heptacyanomolybdates(IV). The appearance of these bands indicates that the reaction with dioxygen results in the oxidation of molybdenum(II) to molybdenum(IV) species with subsequent partial decomposition and cyano ligands release. Such an interpretation is also confirmed by spectral changes induced by the addition of KCN excess to an oxidized solution of **1** (part c of Figure 6). The observed reaction leads to a decrease of the band at 500 nm accompanied by the formation of new bands at 367 and 427 nm, typical for the $[Mo(CN)_8]^{4-}$ anion. This reaction does not affect the band at 630 nm corresponding to tetracyanooxomolybdates(IV), which is in agreement with the fact that they are relatively stable under these conditions. The presence of an isosbestic point at 446 nm additionally confirms the explanation.

Thermogravimetric Measurements. Thermogravimetric measurements combined with a quadrupole mass spectrometry indicate that a decomposition process of salt **1** begins almost at room temperature (Figure 7). This explains the instability of **1** mentioned earlier and problems with its elemental analysis. Analysis of gases evolving during thermolysis shows that NH_3 molecules are released in the first step (up to 250 °C). The loss of mass in this step (3.44%) is close to that calculated for a corresponding amount of N_2H_4 present in **1** (3.17%). Further decomposition, observed above 300 °C, is associated with a stepwise cyano ligands release. This process results in the formation of HCN and $(CN)_2$, detected by mass spectrometry.

Cyclic Voltammetry Measurements. The electrochemical properties of **1** were investigated in aqueous solutions using cyclic voltammetry measurements. In the studied range (−600 to 1200 mV), four oxidation and three reduction peaks are observed (part a of Figure 8). Each peak was measured separately at different scan speeds to confirm its origin and reversibility.
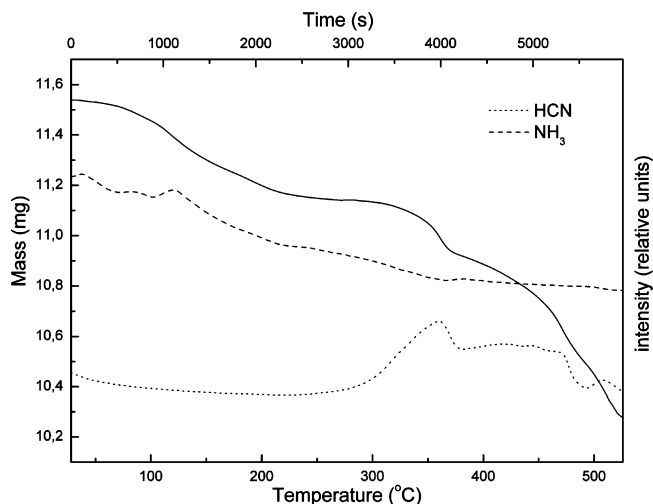
Figure 7. Thermogravimetric curve for $K_5[Mo(CN)_7]\cdot N_2H_4$ (**1**) (solid line) with NH_3 and HCN signals in mass spectrometry.
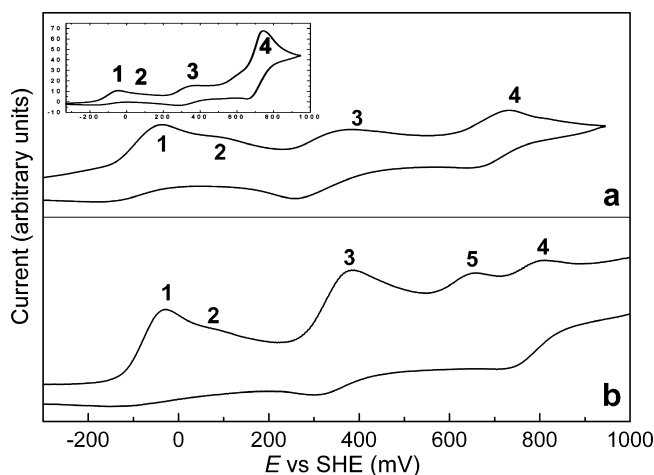
Figure 8. (a) Cyclic voltammetry of $K_5[Mo(CN)_7]\cdot N_2H_4$ (**1**) in 0.10 M KNO_3, scan speed 100 mV/s. In the left upper corner the voltammogram after addition of $K_4[Mo(CN)_8]\cdot 2H_2O$ is shown for comparison. (b) Cyclic voltammetry of **1** in 0.10 M KCN (scan speed 100 mV/s).

At a first glance, peak 1 seems to be associated with an irreversible oxidation process because its corresponding reduction wave is not well resolved. However, the oxidation potential shows only little dependence on a scan speed; it shifts from 7 to 54 mV upon a 100 to 1000 mV/s scan-speed change. This indicates that the observed irreversibility is a result of a chemical reaction that follows the electro-chemical oxidation. The process associated with peak 1 can be attributed to the oxidation of molybdenum(II) to molybdenum(III) moieties. The unknown molybdenum(III) heptacyano complex undergoes fast decomposition, which accounts for the lack of the reduction wave (part a of Figure 8).

It has been observed that shoulder 2 at 127 mV (100 mV/s) disappears with repeated scanning, whereas all other peaks (1, 3, 4) remain unaltered. This peak is associated with transient decomposition products of unstable molybdenum(III) species, formed at lower potential as evidenced in measurements with excess of KCN described below. The positions of both oxidation and reduction waves (peak 3) remain unchanged within 50−1000 mV/s scan speed range,

the corresponding half-wave potential, $E_{1/2}$, is equal to 380 mV. The presence of oxidation and reduction peaks, the independence of $E_{1/2}$ on scan speed, and the symmetry of anodic and cathodic peaks ($I_a/I_c = 0.98$ at 100 mV/s) indicate a reversible process. The anodic and cathodic peak separation (86 mV at 100mV/s) correlates well with a one-electron process attributed to a molybdenum(III)/molybdenum(IV) system.

The oxidation peak 4, observed in the 700−1000 mV range, has the corresponding reduction wave and the calculated $E_{1/2}$ equal to 0.780 V (part a of Figure 8). The anodic and cathodic peak separation is 59 mV, which is a value typical for a one-electron process. This redox process does not seem to be fully reversible, but it has been observed that the addition of $K_4[Mo(CN)_8]\cdot2H_2O$ to the studied solution results in an increase of peak 4 (inset in part a of Figure 8). Thus, it is attributable to the $[Mo(CN)_8]^{3-}/[Mo(CN)_8]^{4-}$ redox couple (with $E°$ equal to 0.78 V).[22] The ill-defined reduction wave is caused by the fact that the strongly oxidizing $[Mo(CN)_8]^{3-}$ anion oxidizes CN^- ions present in solution. The assignment of peak 4 for the $[Mo(CN)_8]^{3-/4-}$ redox couple was additionally corroborated with cyclic voltammetry measurements for pure $K_4[Mo(CN)_8]\cdot2H_2O$ under similar conditions. The reversible one-electron $[Mo(CN)_8]^{3-/4-}$ redox system (with the same $E_{1/2}$, E_a, and E_c values as peak 4) after the addition of small amounts of KCN shows the same behavior as the studied system in part a of Figure 8 (with unsymmetrical oxidation and reduction peaks).

The cyclic voltammogram for **1** in 0.10 M aqueous KCN solution is presented in part b of Figure 8. In general, a recorded curve is similar to that observed for **1** in a 0.10 M aqueous KNO_3 solution (part a of Figure 8). The significant difference is the formation of a new peak (peak 5) at a lower potential (0.656 V) than that of the $[Mo(CN)_8]^{3-/4-}$ redox couple. Similarly, as in the measurements with a nitrate electrolyte, the addition of $K_4[Mo(CN)_8]\cdot2H_2O$ results in an increase of peak 4, which is in agreement with its previous assignment. The addition of $[Mo(CN)_4O(L)]^{n-}$ anions (L = OH^-, CN^-, or NH_3) together with test cyclic voltammetry measurements of $K_3Na[Mo(CN)_4O_2]\cdot6H_2O$ in 0.10 M KNO_3 or 0.10 M KCN indicate that peak 5 is attributable to the oxidation of tetracyanooxomolybdate(IV). Because tetracyano complexes of molybdenum can exist in the form of either $[Mo(CN)_4O(OH)]^{3-}$ or $[Mo(CN)_4O(H_2O)]^{2-}$ (depending on pH, $pK = 9.7$) common formula, $[Mo(CN)_4O(L)]^{2-}$, was introduced. The tetracyano complex exists also in equilibrium with $[Mo(CN)_5O]^{3-}$ and $[Mo(CN)_6]^{2-}$ ions. However, under studied conditions a tetracyano- complex is a predominant species.[13a] The presence of tetracyanooxomolybdates(IV) in solution of **1** confirms that decomposition processes occurring at potentials higher than peak 1 (part b of Figure 8) result in formation of complexes with a lower number of cyano ligands, which, under an excess of CN^- ions, convert into

tetracyanooxomolybdates(IV) accountable for the appearance of peak 5.

Cyclic voltammetry findings on redox processes occurring in $[Mo(CN)_7]^{5-}$ aqueous solutions can be illustrated with eqs (4−11):

$$\text{peak 1: } [Mo^{II}(CN)_7]^{5-} \rightarrow [Mo^{III}(CN)_7]^{4-} + e^- \quad (4)$$

$$[Mo^{III}(CN)_7]^{4-} \rightarrow [Mo^{III}(CN)_x]^{(x-3)-} + (7-x)CN^- \quad (5)$$

$$\text{peak 2: } [Mo^{III}(CN)_x]^{(x-3)-} \rightarrow [Mo^{IV}(CN)_x]^{(x-4)-} + e^- \quad (6)$$

$$[Mo^{IV}(CN)_x]^{(x-4)-} + (4-x)CN^- + L + OH^- \rightarrow$$
$$[Mo^{IV}(CN)_4O(L)]^{n-} + H^+ \quad (7)$$

$$\text{peak 3: } [Mo^{III}(CN)_7]^{4-} \rightarrow [Mo^{IV}(CN)_7]^{3-} + e^- \quad (8)$$

$$[Mo^{IV}(CN)_7]^{3-} + CN^- \rightarrow [Mo^{IV}(CN)_8]^{4-} \quad (9)$$

$$\text{peak 4: } [Mo^{IV}(CN)_8]^{4-} \rightarrow [Mo^{V}(CN)_8]^{3-} + e^- \quad (10)$$

$$\text{peak 5: } [Mo^{IV}(CN)_4O(L)]^{n-} \rightarrow [Mo^{V}(CN)_4O(L)]^{(n-1)-} + e^- \quad (11)$$
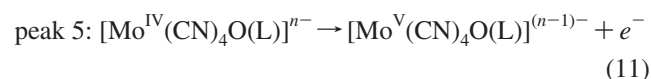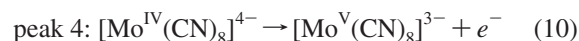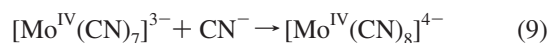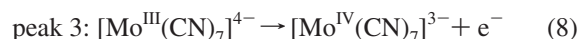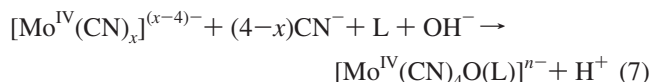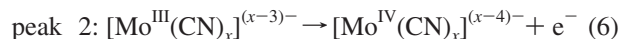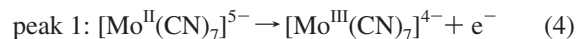
where $L = H_2O$, OH^- or CN^-.

The cyclic voltammogram presented in part a of Figure 8 indicates that dissolving of **1** and its subsequent electrochemical oxidation or reduction result in a release of cyano ligands and a formation of numerous products. Most of those products were recognized and attributed to octa- and heptacyano ions undergoing redox processes. The formation of octacyanomolybdates(IV) from heptacyano complexes indicates a presence of free CN^- ions in solution and their coordination upon oxidation to hepacyanomolybdate. Thus, complexes with a number of cyano ligands lower than seven must be formed, but these are not observed in voltammograms (except for a transient peak 2). The lack of the peak 5 in part a of Figure 8, attributable to tetracyano complexes and its appearance upon KCN addition indicate a cyanation process. Thus, it is reasonable to suggest a presence of complexes with less than four cyano ligands per molybdenum center. Up until now, there are not any representatives of monomeric molybdenum complexes of this type. Only were the trimeric $[Mo_3O_4(CN)_{9-x}(H_2O)_x]^{n-}$ complexes reported, but these were isolated in much more acidic conditions.[23] The complex accountable for the formation of a transient peak 2 in the voltammogram cannot be attributed to any of the isolated earlier cyano complexes of molybdenum, and thus eqs 5−8 contain complexes with an unspecified number of cyano ligands, x.

Catalytic Decomposition of Hydrazine. As it was shown earlier, the irradiation of $K_4[Mo(CN)_8]\cdot2H_2O$ in $N_2H_4\cdot H_2O$ results in quantitative N_2 and NH_3 formation according to an overall equation:

$$3N_2H_4 \rightarrow N_2 + 4NH_3 \quad (12)$$
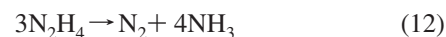
The detailed study shows that N_2H_4 can be totally converted into N_2 and NH_3, and the amount of formed products is only limited by the starting amount of N_2H_4.

(22) Szklarzewicz, J.; Samotus, A.; Kanas, A. *Polyhedron* **1986**, *11*, 1733–1740.

(23) Szklarzewicz, J.; Samotus, A. *Polyhedron* **1993**, *12*, 1471–1475.

Thus, hydrazine is catalytically decomposed in the presence of molybdenum complexes during photolysis. The calculated turnover numbers (as moles of hydrazine consumed per one mole of starting [Mo(CN)$_8$]$^{4-}$ complex) exceed 10^3, and we did not aim in determining its upper limit.

The formation of **1** in the reaction:

$$[Mo^{IV}(CN)_7]^{3-} + 1/2N_2H_4 \rightarrow [Mo^{II}(CN)_7]^{5-} + 1/2N_2 + 2H^+ \quad (13)$$
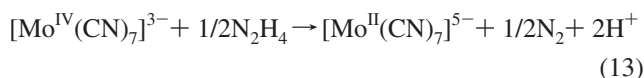
was confirmed by the measurements of N$_2$ and NH$_3$ released at the very early stage of photolysis. The irradiation of K$_4$[Mo(CN)$_8$]·2H$_2$O (0.1173 g) in N$_2$H$_4$·H$_2$O (0.50 mL) until light-green color appears, gives the molar ratio Mo/N$_2$/NH$_3$ equal 1.2/1/1, which means a 4-fold increase of the amount of N$_2$ compared to that expected from (12). The formation of H$^+$ ions (13) was ascertained through pH measurements, which reveal that pH of irradiated solutions decreases rapidly and comes close to 5.6 once the [Mo(CN)$_7$]$^{5-}$ complex has been formed. Upon further irradiation, the solution turns deep green. At this stage, our attempts to isolate pure products were unsuccessful. However, when the green solution was dried under vacuum the resulting residue was found to be paramagnetic. The green residue has ESR, IR, and UV−vis spectra (peak positions) similar to those of molybdenum(III) cyano complexes described in the literature.[21,24,25] However, the residue is likely to be a mixture of products, thus it is not possible to determine the molar extinction coefficients (in the UV−vis spectra). It can be assumed that the molybdenum(III) complex is formed in the reaction:

$$2Mo^{2+} + N_2H_4 + 2H^+ \rightarrow 2Mo^{3+} + 2NH_3\uparrow \quad (14)$$
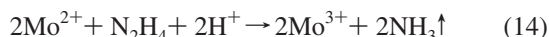
The further photolysis of the green solution does not affect the UV−vis spectrum of the solution, but the intense evolution of N$_2$ and NH$_3$ gases is observed at this stage. At the end of photolysis, when hydrazine is nearly completely decomposed, the concentrated NH$_3$(aq) solution is formed, and the solution turns blue due to the formation of [Mo(CN)$_4$O(NH$_3$)]$^{2-}$ according to the reaction:

$$2Mo^{3+} + N_2H_4 + 2H^+ \rightarrow 2Mo^{4+} + 2NH_3\uparrow \quad (15)$$
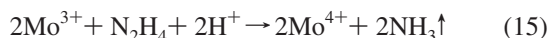
To study the activity of primary, transient, and final photoproducts, the rate of N$_2$ formation during photolysis was measured and it is presented in Figure 9. The activity presented in Figure 9 represents a thermal (and not a photochemical) activity of the series of equimolar [Mo(CN)$_8$]$^{4-}$ solutions, each irradiated for a certain period of time before being subjected to an analysis. This activity refers to all photoproducts present in each solution after irradiation is stopped. The procedure described in the Experimental Section allowed us to avoid the influence of photochemical processes on the thermal catalytical activity of photoproducts.

It can be clearly seen that the catalytic activity increases during photolysis with the maximum at the stage of the green

(24) Rossman, G. R.; Tsay, F. D.; Gray, H. B. *Inorg. Chem.* **1973**, *12*, 824–829.
(25) Mockford, M. J.; Griffith, W. *J. Chem. Soc., Dalton Trans.* **1985**, 717–722.
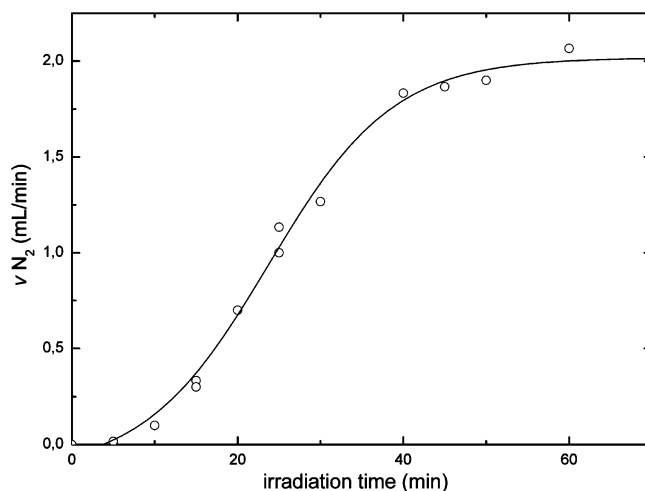
Figure 9. Rate of N$_2$ formation versus irradiation time (at 90 °C).

solution (irradiation time >40 min). At this stage, the activity toward N$_2$H$_4$ remains constant up until its almost total decomposition.

The observed thermal catalytic activity was compared with that of K$_4$[Mo(CN)$_8$]·2H$_2$O and isolated photoproducts (including **1**, **2**, [Mo(CN)$_4$O(NH$_3$)]$^{2-}$, [Mo(CN)$_5$O]$^{3-}$, and [Mo(CN)$_4$O(OH)]$^{3-}$) under the same conditions. It has been shown that the [Mo(CN)$_8$]$^{4-}$ ion is catalytically inactive, whereas salts **1** and **2** show activity at the level of 0.13 mL N$_2$/min. This value is in agreement with the data presented in Figure 9 because **1** is being formed up until 10 min of irradiation, under studied conditions.

The solutions containing [Mo(CN)$_4$O(L)]$^{n-}$ ions (L = CN$^-$, OH$^-$, NH$_3$) dissolved in N$_2$H$_4$·H$_2$O (98%), independently on L, turn dark green upon temperature increase, and show activity at a level of 2.0 mL N$_2$/min. This observation confirms that the final photoproducts are the most active complexes, which can be easily converted into a molybdenum(III) species in a strongly reducing medium. The activity of tetracyanooxomolybdates(IV) is the same as that observed within a plateau in Figure 9, which indicates the same origin of active centers in both photolyzed and nonphotolyzed systems.

The photolysis affords molybdenum(II) complex (eq 13), which is subsequently oxidized to molybdenum(III) species (eq 14). This low-cyano molybdenum(III) product participates in a catalytic cycle, involving molybdenum(IV) complex, represented by reactions (15) and (16).

$$4Mo^{4+} + N_2H_4 \rightarrow 4Mo^{3+} + N_2 + 4H^+ \quad (16)$$
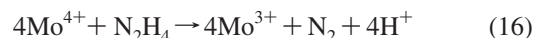
Thus, in the catalytic cycle, we observe a reduction of the molybdenum(IV) complex with the indication of a molybdenum(III) species formation and its reoxidation to the molybdenum(IV) complex. The same cycle can be observed when reaction with hydrazine begins directly from tetracyanooxomolybdates(IV) and not via the photolytical route. Because the redox cycle can be achieved starting from [Mo(CN)$_4$O(L)]$^{n-}$ ions, it can be assumed that N$_2$H$_4$ replaces labile ligand L, and then the resulting complex can be reduced, yielding coordinatively unsaturated molybdenum(III) species (eq 16). The latter can oxidize N$_2$H$_4$ to NH$_3$

Scheme 1. Molybdenum-Based Catalytic Decomposition of Hydrazine

$$[Mo^{IV}(CN)_8]^{4-}$$

$$\downarrow h\nu$$

$$*[Mo^{IV}(CN)_8]^{4-}$$

$$-CN^- \Big\Uparrow +CN^-$$

$$[Mo^{IV}(CN)_7]^{3-}$$

$$\Bigg\downarrow \nearrow 1/2N_2H_4$$
$$\searrow 1/2N_2 + 2H^+ + 2e^-$$

$$[Mo^{II}(CN)_7]^{5-}$$

$h\nu$ *or* temp $\diagup\diagdown$ $1/2N_2H_4 + H^+ + e^-$

$CN^- \diagdown\diagup NH_3$

Mo^{III} species

$1/4N_2 + H^+ + e^- \diagleft$ $\diagright 1/2N_2H_4 + H^+ + e^-$

$1/4N_2H_4$ $[Mo^{IV}(CN)_4O(L)]^{n-}$ NH_3
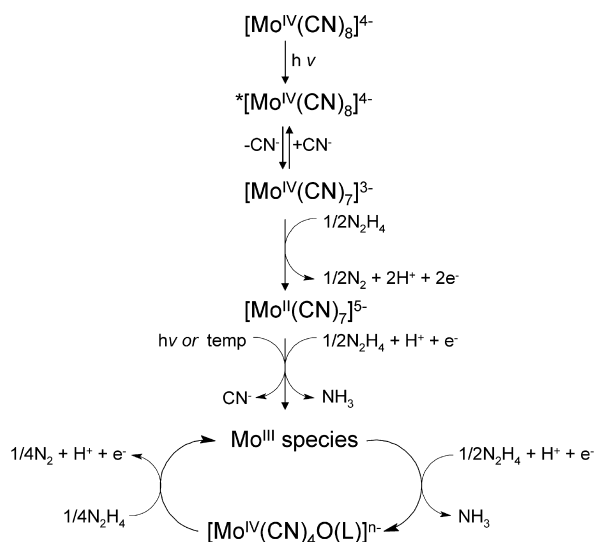
with accompanying recovery of the molybdenum(IV) complex. The overall molybdenum-based catalytic mechanism of N_2H_4 decomposition is presented in Scheme 1.

Concluding Remarks. For the first time, we have been able to obtain an efficient catalytic system based on molybdenum(III/IV) cyano complexes. It has been shown that in strongly reducing media it is possible to reduce both primary and final photoproducts of $[Mo(CN)_8]^{4-}$ photolysis and to isolate an unstable molybdenum(II) intermediate. The produced molybdenum(II) species can reduce N_2H_4, yielding molybdenum(III) and molybdenum(IV) complexes that can be further reduced by N_2H_4, thus closing the catalytic cycle, whose turnover number exceeds 10^3. There is strong evidence of low activity of the molybdenum(II) and high activity of the molybdenum(IV) complexes. The same catalytic cycle can be achieved in a thermal way, starting from tetra- or penta-cyano complexes of molybdenum(IV). There are also strong indications of a presence of molybdenum(III) during the catalytic cycle. It also seems that proper modifications of the system could make these complexes act as competitive catalysts with nitrogenase-like activity, which will be the subject of further investigations. A facile and efficient method of cyanomolybdates(II) synthesis, presented in this article, can also be used for exploration of molybdenum(II) chemistry.